Phytoliths of Amazonian grasses: diversity and applications
Fitolitos de gramíneas amazónicas: Diversidad y aplicaciones

Gaspar Morcote-Ríos[1], Diego Giraldo-Cañas[1,2] & Lauren Raz[1]

[1]Instituto de Ciencias Naturales, Universidad Nacional de Colombia, Bogotá D. C., Colombia.

[2]Corresponding author: dagiraldoc@unal.edu.co.

Orcid id: 0000-0003-0212-7489.

Recibido: 01-10-2024

Aprobado: 06-01-2025

Publicado: 31-03-2025

Artículo de investigación

Abstract

In the Poaceae, silica accumulates in idioblast cells in leaves and other organs, forming bodies called "grass silica short cell phytoliths" (GSSCP). Epidermal cells and hairs can also accumulate silica and are considered phytoliths as well. The GSSCPs are particularly well studied and can be diagnostic at different taxonomic levels, including subfamily. This, and the fact that phytoliths can persist in soils for millions of years, make them useful proxies to characterize plant assemblages in paleoecological and archaeological studies. Over the past decade we have been developing phytolith reference collections of Amazonian taxa to aid in the identification of ancient plant remains from this region. To create a representative Amazonian grass collection, we extracted phytoliths from 150 species (88% of Colombian Amazonian grasses) in 59 genera and seven subfamilies. We identified 12 broad morphotype categories with a total of 54 variants, partitioned into two datasets: GSSCP and other silicified epidermal structures; UPGMA analyses were conducted to test for groupings at subfamily level in the separate and combined datasets. We found diagnostic morphotypes at the genus or even species level in some cases, and also identified silicified epidermal cells in both archaeological and paleoecological samples; however, we found no clear pattern of morphotype distribution at subfamily level, a result that contrasts with GSSCP surveys from other regions. We reiterate calls for more intensive regional sampling to elucidate patterns of variation in both GSSCP and other silicified epidermal structures in grasses.

Key words: Amazonian archaeology; Amazonian paleoecology; Neotropical grasses; phytolith morphotypes.

Resumen

En las gramíneas, el sílice se acumula en idioblastos en las hojas y otras estructuras, constituyendo cuerpos denominados "fitolitos de sílice de gramíneas en células cortas" (GSSCP). Las células epidérmicas y los tricomas también pueden acumular sílice y éstos también se consideran fitolitos. Los GSSCP están bien estudiados y pueden ser diagnósticos en diferentes niveles taxonómicos, incluídas las subfamilias. Esto y el hecho de que los fitolitos pueden persistir en los suelos durante millones de años, hacen de éstos "*proxies*" útiles para caracterizar arreglos vegetales en estudios paleoecológicos y arqueológicos. Nosotros hemos desarrollado en la pasada década, colecciones de referencia de fitolitos de diferentes taxones amazónicos, con el objetivo de ayudar en la identificación de restos vegetales de esta región. Así, para crear una colección representativa de gramíneas amazónicas, extrajimos fitolitos de 150 especies (88% de las gramíneas amazónicas colombianas), distribuidas en 59 géneros y siete subfamilias. Identificamos doce categorías de morfotipos de fitolitos con un total de 54 variantes, divididos en dos grupos de datos: Los GSSCP y otras estructuras epidérmicas silicificadas. Empleamos análisis UPGMA con el fin de probar las agrupaciones de los fitolitos a nivel de subfamilia, por separado y también combinando conjuntos de datos. Encontramos morfotipos de fitolitos diagnósticos a nivel de género, y en algunos casos, a nivel de especie. Asimismo, pudimos identificar células epidérmicas silicificadas en muestras arqueológicas y paleoecológicas. No obstante, no encontramos un claro patrón de la distribución de los morfotipos al nivel de subfamilia, un resultado que contrasta con los hallazgos de GSSCP para otras regiones. Así, hacemos hincapié en la necesidad de adelantar más muestreos regionales, con el fin de dilucidar los patrones de variación, tanto en GSSCP como en otras estructuras epidérmicas silicificadas en gramíneas.

Palabras clave: Arqueología amazónica; gramíneas neotropicales; morfotipos de fitolitos; paleoecología amazónica.

Introduction

Phytoliths are microscopic structures composed of hydrated silica (SiO_2 * nH_2O) that accumulates in the tissues of diverse plant taxa as well as in some unicellular eukaryotes (Prychid *et al.*, 2003). They are especially abundant in commelinid monocots, and in grasses they form two distinct groups of structures; the best described are the so-called grass silica short cell phytoliths (GSSCP), which are formed in idioblast cells in horizontal or vertical arrays in the epidermis of leaves and other organs (Piperno, 2006; Strömberg, 2018). These present morphologies that are often diagnostic at or below subfamily level (Twiss, 1969; Piperno & Pearsall, 1998; Rudall *et al.*, 2014; Neumann *et al.*, 2017). To date, research has focused mostly on GSSCPs, but other epidermal structures in grasses may also become completely filled with silica, including bulliform cells, stomata, hairs and

prickles. These are also considered phytoliths in the broader sense (Zucol, 1998, 2000) and Strömberg (2018) discusses their utility, when examined collectively in sediments, as a proxy to interpret environmental conditions of a given study site. Both she and Piperno (2006) emphasize that individually these structures are of little diagnostic value, but to date, most grass phytolith studies have focused on GSSCPs, while other types of grass phytoliths have received far less attention. Nevertheless, microscopic leaf epidermal characters have long been recognized as being of taxonomic utility, (Prat, 1932; Ellis, 1979; Palmer & Tucker, 1981; Londoño & Kobayashi, 1991; Khan *et al.*, 2017), which suggests that grass epidermal phytoliths might be of greater utility than is generally appreciated.

Because phytoliths can persist in sediments for millions of years, they can be used to address a great variety of research questions in paleoecological (reviewed in Strömberg, 2018) and archaeological studies (reviewed in Piperno, 2006). Grass phytoliths are of particular interest because pollen is homogeneous in the family, whereas phytoliths are both abundant and highly diverse. Because GSSCP morphotypes are often diagnostic at subfamily level (Piperno, 2006; Bremond *et al.*, 2008; Strömberg, 2018), they are particularly useful in paleoenvironmental studies, where being able to distinguish C_3 from C_4 grasses of the PACMAD clade permits inferences about ancient climates. A high ratio of grass to eudicot phytoliths at a given study site is generally used to infer open habitats, which may in turn be associated with changes in land use (in archaeological contexts) or changes in vegetation cover due to climate or other non-anthropic factors (paleoecological contexts), while finer taxonomic resolution is often desireable in other kinds of studies. For example, grass phytoliths have been used to study domestication of rice (Whang *et al.*, 1998; Zhao *et al.*, 1998; Hilbert *et al.*, 2017) and wheat (Ball, 1999) and to reconstruct ancient diets in hominids and other vertebrate species (Strömberg, 2006; Henry *et al.*, 2012).

In our region of interest, the Amazon, there are several active areas of research for which phytoliths are providing relevant datasets. By comparing contemporary, archaeological and paleoecological data, it should be possible to understand the extent of human impacts on the Amazon during the last 10,000 years (Ferreira *et al.*, 2019; McMichael & Bush, 2019). Phytoliths can also inform studies of vegetation changes in deeper time, including the formation of the Amazon itself (Piperno, 1997; Hoorn *et al.*, 2017, 2022). The Poaceae component of the vegetation is particularly valuable for interpreting changes at both local and landscape scales.

Contrary to popular perceptions, the Amazon is not a homogeneous tropical rain forest, but a patchwork of different vegetation and soil types (Richards, 1996) including granitic outcrops and white sands associated with the Guayana Shield, and grass diversity

in the region is correspondingly complex: we calculate 452 species in seven subfamilies, including both C_3 and C_4 taxa. Panicoideae is by far the most diverse subfamily in the Amazon, with about 2/3 of all species, including both C_3 and C_4 genera. Historically, phytolith studies have focused more on temperate and subtropical grasses, which are predominantly C_3, however in the lowland tropics, the C_4 pathway predominates, and because the panicoids have been particularly undersampled, it is the subfamily with the least well defined phytolith morphotypes (Neumann *et al.*, 2017). Piperno & Pearsall (1998) surveyed phytoliths in approximately 200 species of Neotropical grasses, but only 15% were of Amazonian distribution, and the authors signaled the need for increased regional sampling and increased attention to microscopic features that can be used to separate phytolith morphotypes. Cavalcante (1968) surveyed phytoliths in 25 grass species from the Brazilian Amazon, and hoped one day to produce a catalogue of phytoliths of Amazonian grasses. Unfortunately he did not fulfill this wish, but we recently published an illustrated catalogue of phytoliths of grasses from the Colombian Amazon (Morcote-Ríos *et al.*, 2015). Nevertheless, some important taxa were excluded from that study (native species of *Oryza* and *Streptochaeta*) and we did not assess patterns in the taxonomic distribution of the observed morphotypes.

In the present study, we describe the diversity of phytolith morphotypes from across the spectrum of Amazonian grasses and test the hypothesis that phytoliths are diagnostic at subfamily level in this particular biogeographic context. We also present examples of grass phytoliths obtained from archaeological and paleoecological sediments in the Amazon to highlight the utility of silicified epidermal structures (non GSSCPs) in this region.

Materials and methods

Phytolith extraction from contemporary grass specimens. For this study we evaluated phytoliths in Amazonian grasses corresponding to 7 subfamilies, 59 genera, and 150 species (88% of Colombian Amazonian grasses), sampled from the National Colombian Herbarium (COL), following confirmation of the determinations. Complete voucher information for the specimens is included in Morcote-Ríos *et al.* (2015); we also prepared seven additional samples from four species, including two new genera and one subfamily (Anomochlooideae) that were not included in the previous work. Voucher information for the newly included COL samples is as follows: *Oryza grandiglumis*: Giraldo-Cañas 3641 (leaf), Duque-Jaramillo 2025 (leaf and spikelets); *Oryza latifolia*: Cuatrecasas 10873 (leaf); *Streptochaeta spicata*: Smith 1530 (leaf), Black 51-12891 (leaf); *Streptogyna americana*: Giraldo-Cañas 2590 (leaf). The study includes 22 species that were introduced and have become naturalized in the Amazon during the last 500 years. Fourteen of the specimens sampled were from extralimital collections; these were

chosen in cases where the Amazonian specimens did not have enough material for destructive sampling. Although the specimens may have come from other lowland regions (e.g. *Dinebra panicea* and *Leptochloa virgata*), the species are nevertheless part of the Amazonian grass flora. This study considers a third of all Amazonian grasses and the sampling is representative at genus and subfamily levels, following the classification of Soreng *et al.* (2017). We followed the protocols for phytolith extraction from contemporary herbarium material as described in Morcote-Ríos *et al.* (2015). In most cases, only leaf tissue was sampled (always the last leaf before the inflorescence), but for culturally important species such as maize, *guadua* and sugar cane, culms and inflorescences were also included.

Phytolith extraction from archaeological and paleoecological sediments. Phytoliths were recovered from a sediment sampled collected at the locality of La Sardina (Amazonas, Colombia), associated with a *Terra Preta* (Amazonian Dark Earth) site with a chronology of 1000 years BP (Kalin-Arroyo, M. *et al.*, unpubl. data), and from a paleoecological sediment sample collected from a riverbank at the locality of Santa Sofía 3-91 (Amazonas, Colombia), of Miocene age, between 15 and 12 Ma (Hoorn, C., unpubl. data). The preparation of the sediment samples was adapted from the protocols of Piperno (1988, 2006) and Pearsall (1989). A volume of 1 ml of compact sediment from each sample was manually ground with a mortar to obtain a fine grain sediment. The samples were then treated with 200 ml of 50% hydrogen peroxide to eliminate all organic matter. This action was repeated five times until the solution became clear, indicating digestion of the organic matter. The samples were then subjected to three rounds of centrifugation at 2000 rpm during 5 min., the first two rounds in 90% EtOH and the final round in distilled water in order to eliminate all traces of the peroxide. The phytoliths were then extracted using zinc chloride ($ZnCl_2$) with a density of 2.1, and centrifuged at 500 rpm for 5 min. to separate the light and heavy fractions. The light fraction containing the phytoliths was decanted into labelled microtubes and then mounted onto glass slides in triplicate. The phytoliths were identified via comparison with the contemporary reference collection of the Instituto de Ciencias Naturales at Universidad Nacional de Colombia (ICN, 2019), and Morcote- Ríos *et al.* (2015).

For both the contemporary and ancient samples, description and photography of the phytoliths were carried out using a Nikon Eclipse 400 microscope and an Omni VID LW Scientic digital camera. Although the structures are represented here two-dimensionally, they were observed and described from multiple focal planes. During image processing, the following functions were applied in Adobe Photoshop CS5: noise reduction, autocontrast and automatic color adjustment. The terminology employed here for describing phytoliths and other anatomical structures is based on Ellis

(1979), Zucol (1992, 2000), Gallego & Distel (2004), and Madella *et al.* (2005).

Cluster Analyses. Homology assessment in grass phytoliths is not straight forward (Rudall *et al.*, 2014) and definition of characters and character states remains subjective. Given the nature of the data we chose a clustering method for pattern detection (Neumann *et al.*, 2017; Zucol, 1998, 2000). Once the morphotypes were described, they were coded as present or absent for all 150 species in the dataset. In order to detect patterns at subfamily level, we used UPGMA cluster analysis based on the Sørensen-Dice similarity index (qualitative), implemented in the PAST3 statistics package. We analyzed a combined matrix of both GSSCP and silicified epidermal structures following Zucol (1998, 2000), and also partitioned the data into two matrices (GSSCP only and Silicified Epidermal Structures only), which were analyzed separately under the same parameters.

Results

Diversity of phytolith morphotypes in contemporary Amazonian grasses. Across the entire sample of 150 Amazonian grass species, we recognized 54 phytolith morphotypes that we grouped into 12 broad categories (Figs.1, 2, 3). These include seven GSSCP categories with 32 variants and five categories of silicified epidermal structures with 22 variants. The taxonomic distribution of the morphotypes is presented in Table 1 and the schematic 2-D illustrations of all the variants are presented in Fig. 1, which also includes brief descriptions in the caption. We have assigned letter names to the 54 variants and these were the morphotypes that were coded in the cluster analysis (below), but several of the variants actually have subvariants (e.g. Fig. 1U, W, HH, PP, YY, ZZ). Within a highly variable group like U for example, all subvariants share the same basic geometry but with subtle differences in degrees of curvature/concavity. Had we chosen to elevate each subvariant, we could have recognized as many as 95 variants. These are the sorts of subjective decisions that make comparison among studies by different authors difficult, an issue raised by Neumann *et al.* (2017). In this case we opted to reduce the number of categories to make comparisons easier. Consistent with other authors (Piperno & Pearsall, 1998; Neumann *et al.*, 2017), we recognized variation in the length of the center or shaft (= shank of Neumann *et al.*, 2017) of bilobate forms, and the presence of convexities and/or concavities in the lobes, as well as variations in the length and/or degree of curvature of the edges in the other morphotypes.

Contrary to our expectations, we did not recover clear patterns of morphotype distribution at the subfamily level, with two notable exceptions in Chloridoideae and Pharoideae. See Cluster Analyses, below for more results at subfamily level (Figs. 4, 5, 6). Nevertheless, we did find diagnostic morphotypes for certain genera and species in the Amazon and these are detailed below. They

include both GSCCPs and silicified epidermal structures and are listed here in order of the categories as they are presented from left to right in Table 1. Consult Fig. 1 for illustrations and descriptions of the diagnostic variants.

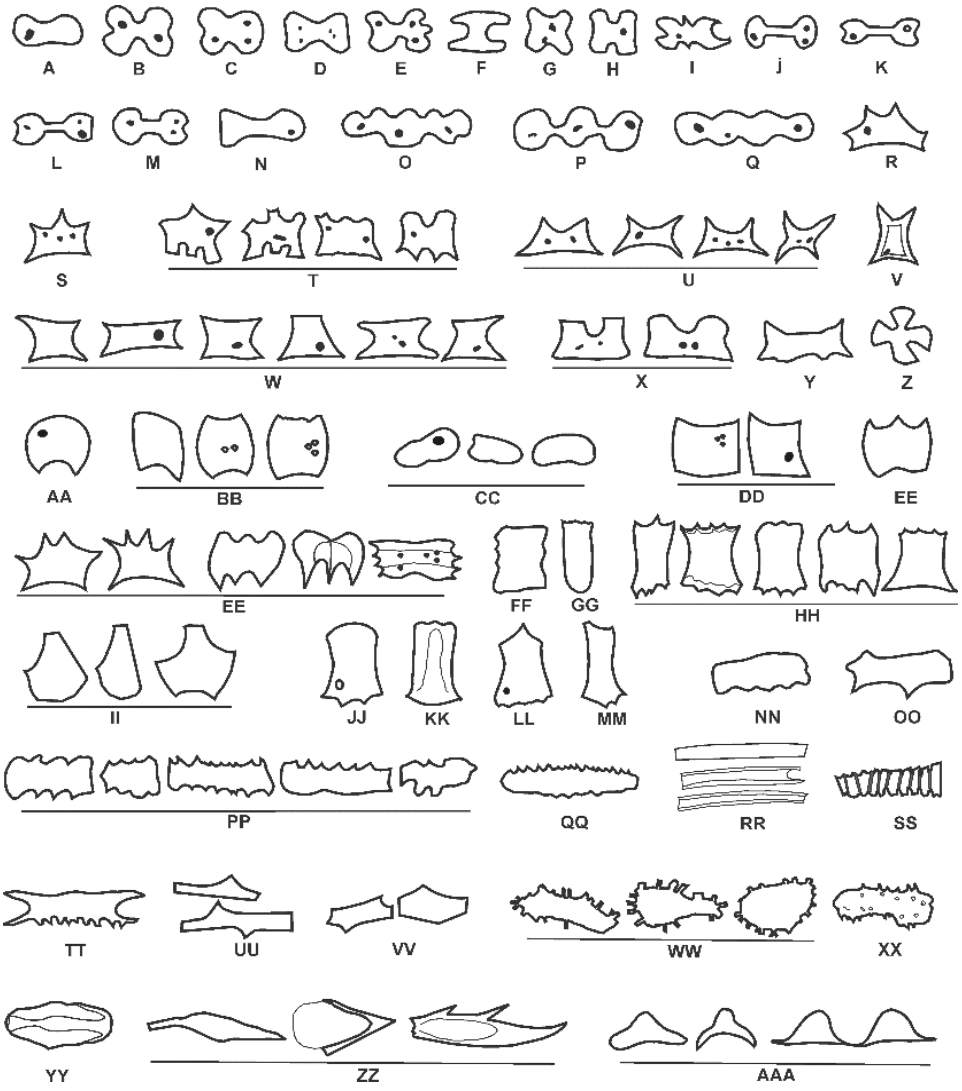

Figure 1.

Bilobate short cell (A-I). A, convex ends. Longest axis: 9.8-21.5 µm. **B**, concave ends. Longest axis: 5.8-31.3 µm. **C**, convex-concave ends. Longest axis: 15.6-24.5 µm. **D**, straight-concave ends. Longest axis: 11.7-17.1 µm. **E**, concave ends and rome projection. Longest axis: 24.5 µm. **F**, Bilobate with short center and convex ends. Longest axis: 17.6-19.6 µm. **G**, concave ends and

thick center; “thick cross” of Piperno & Pearsall (1998). Longest axis: 10.7-15.6 µm. **H**, quadrangular. Longest axis: 11.7 µm. **I**, acute projections and convex ends. Longest axis: 19.6-22.5 µm. **Bilobate long cell (J-N)**. **J**, convex ends. 20.5-41.4 µm. **K**, concave ends. Longest axis: 17-45.6 µm. **L**, straight-concave ends. Longest axis: 16.6-23.5 µm. **M**, convex-concave ends. Longest axis: 20.5-24.5 µm. **N**, straight- convex ends. Longest axis: 18.6-19.6 µm. **Polylobate (O-Q)**. **O**, longest axis: 22.5-53.9 µm. **P**, longest axis: 17.6-45.6 µm. **Q**, longest axis. 25.4-29.4 µm. **Trapezoidal (R-Y)**. **R**, longest axis: 39.2 µm. **S**, longest axis: 9.8-48 µm. **T**, longest axis: 22.5-48 µm. **U**, trapezoidal concave base. Long. Base: 3.4-23.5 µm. **V**, longest axis: 11.7 µm y 15 µm. **W**, trapezoidal flat base. Long. Base: 10.7 µm and 24.5 µm. **X**, longest axis: 11.7-27.4 µm. **Y,** trapeziform with sinuate base and double peaks. Longest axis: 42.1 µm. Height: 19.6 µm. **Z**, cross. Longest axis: 14 µm. **Suborbicular-rectangular (AA-DD)**. **AA**, suborbicular with concave area. Longest axis. 10.7 µm. **BB**, rectangular with two opposite sides concave and the others convex (Saddle). **CC**, longest axis. 9.8 µm. **DD**, longest axis: 13 µm. **Carinate**. **EE**, different views. Presents several acute projections in lateral view. Caracterized by carinate (crest-like) structures. Present in very few species, but at especially high density in *Trichanthecium polycomun*. **Bulliform Cell**. (**FF-MM)**. **FF**, longest axis: 24.5 µm. **GG**, longest axis: 48 µm. **HH**, longest axis: 24.5-52.8 µm. **II**, longest axis: 39.2-69.6 µm. **JJ**, longest axis: 22 µm. **KK**, longest axis: 24-52 µm. **LL**, longest axis: 36 µm. **MM**, longest axis: 45 µm. **Elongate epidermal cell (NN-VV). NN**, longest axis: 11.2-15.5 µm. **OO**, long, thick epidermal cell with one or few acute projections along one margin: Longest axis: 20-36 µm. **PP**, long, thick epidermal cells with serrate and/or ondulate margins. Longest axis: 11.7-50.9 µm. **QQ**, long, thick epidermal cells with serrate and/or ondulate margins and ends rounded, the structure symmetrical. Longest axis: 115.2 µm. **RR**, long, thin epidermal cell with straight margins with simple or double walls. Longest axis: 37.2-98 µm. **SS**, silicified vessel element with parallel divisions. Longest axis: 20.5-96 µm. **TT**, long epidermal cell with concave end. Longest axis: 120 µm. **UU**, elongated epidermal cell with acute marginal projection aguda. Longest axis: 16-144 µm. **VV**, rhomboid epidermical cell. Longest axis: 60 µm. **Amorphous with marginal projections (WW-XX)**. **WW**, amorphous with marginal projections**.** Longest axis: 36-40.1 µm. **XX**, amorphous with short acute projections on the surface, characterized by relatively small size, with variable shapes, found exclusively in the spikelets. Longest axis: 10.78-23 µm. **Misc. epidermal structures (YY-ZZ). YY**, elliptical stomatal complexes. Longest axis: 18.1-48 µm. **ZZ**, bicellular microhair: Longest axis: 19.6-98.4 µm. Epidermal prickle. Longest axis: 14.7-76.8 µm Trichomes: Longest axis: 21.5 µm, Unicellular macrohair: Longest axis 30.3-79.2 µm. **AAA**, **Mammiform-Conical**. Apex suborbicular. Base length: 7.4-18.6 µm.

-In the GSCCP category bilobate short cell, variant I was found exclusively in *Oryza latifolia* (Fig. 2E). It is characterized by having acute central projections and concave lobes and is present at high density in this species. In the same category, variant E was found exclusively in *Paspalum melanospermum* and *Ocellochloa pulchella*.

-In the GSSCP category trapeziform, the variant Y was found only in the spikelets of *Oryza grandiglumis* and variant T is found only in the bambusoids *Olyra latifolia*, and the genera *Piresia, Pariana*, and *Streptochaeta spicata* (Anomochlooideae), while variant V occurs exclusively in the genus *Pariana*.

-In the GSCCP category cross, we identified the unique variant Z in *Piresia goeldii*, characterized by its unusual thickness.

-In the GSSCP category suborbicular-rectangular, the variant BB was found exclusively in the species *Chloris ciliata*, *C. dandyana*, *C. inflata*, *Cynodon dactylon*, *C. nlemfuencis*, *Eleusine indica*, *Eragrostis japonica*, *E. maypurensis*, *E. pilosa*, *E. tenuifolia*, *Leptochloa virgata*, and *Piresia sympodica*, making it a useful marker for Chloridoideae, although *Piresia* stands out from this group as the only bambusoid. In the same category, variant AA was only present in the panicoid *Gynerium sagittatum*. Our variant DD of the same category is diagnostic for the genus *Pharus.* This latter structure was also described in *Pharus* by Piperno (1988, 1998), who remarked at the time that it was an unusual morphotype for a bambusoid grass. In subsequent classifications, *Pharus* has been placed in its own subfamily, and this unique phytolith morphotype could thus be interpreted as an autapomorphy.

-We created a GSCCP category carinate, with a geometry that does not fit neatly in any of the established categories but is characterized by the presence of notorious parallel ridges. This morphotype was observed in *Ocellochloa stolonifera*, *Otachyrium versicolor*, *Streptochaeta spicata* and the genus *Trichanthecium*. In *S. spicata* it is the most abundant morphotype, and previous authors have described it as saddle-like (Piperno & Pearsall, 1998) or irregular (Rudall *et al.*, 2014).

-Elongate epidermal cells of variant UU were found exclusively in the culms (cane) of *Saccharum officinarum*, providing a useful proxy to trace the introduction of this species. -The variant VV of the same phytolith category was only recorded in *Paspalum fasciculatum*.

-The silicified epidermal structure, amorphous with projections, variant WW was only found in culms *Guadua angustifolia*, an ecologically and culturally important Amazonian species. Variant XX of the same category occurred at high density in the spikelets of *Oryza grandiglumis*. This structure is also caracterized by its relatively small size (Fig. 2F).

-Mammiform cells of variant AAA were found in the panicoid species *Coleataenia caricoides* and the bambusoid *Arthrostylidium* sp.

Archaeological and paleoecological samples. In the 1000 year old archaeological sample from La Sardina, the most conspicuous grass phytolith was amorphous with projections, diagnostic for the culms of *Guadua angustifolia* (Table 1). In Fig. 2 we present both the archaeological and contemporary phytoliths of this morphotype in *G. angustifolia*. In the same region today this species is a dominant component of the vegetation, suggesting that there have not been significant changes over the last 1000 years. The association of this species in a human cultural context also suggests that the species may have been used by the local population.

In the paleoecological sample from Santa Sofía grass phytoliths were well represented, including GSSCPs of widespread taxonomic distribution (trapeziform variant U), but the bulliform cell variant II was also common (Fig. 2). We observed this phytolith morphotype in 19 Amazonian species from varied habitats (Table 2), distributed across five subfamilies (Table 1). If we compare the contemporary grass flora of the area with these 19 taxa (Giraldo-Cañas, D, unpubl. data), five genera are shared between the two datasets: *Guadua*, *Gynerium sagittatum*, *Leptochloa, Paspalum*, and *Panicum*. If other elements of the contemporary flora are also found in fossil pollen, seeds, etc., that would suggest that the vegetation in this region has remained fairly stable since the Miocene and would increase confidence in the determination of the phytoliths. We should also note that variant II of the category bulliform cells is actually more complex that what we have represented in Fig. 1 and requires further study. As many as 10 subvariants may be recognized, likely providing an even finer level of taxonomic resolution. Scanning electron microscopy will be particularly useful to capture this level of detail (Fig. 3).

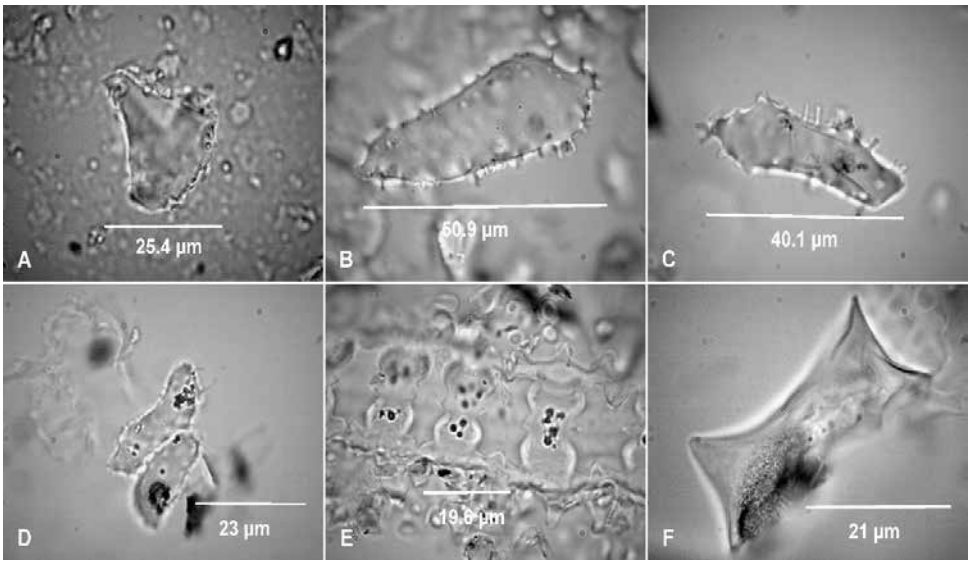

Figure 2.

Phytoliths of Amazonian grasses from paleoecological (A) and archaeological (B) contexts and modern reference collections (C-F). **A**, bulliform cell (variant II) from the Miocene 15-12 My (Colombia. Amazonas: Leticia, Santa Sofía 3-91). **B**, amorphous silicified structures (variant WW) with marginal proyections from *Guadua angustifolia*, associated with *Terra Preta* archaeological site from 1000 BP (Colombia. Amazonas: La Sardina, Middle Caquetá River). **C**, amorphous with fine projections from *Guadua angustifolia* (variant WW), characteristic structures of the culm. **D**, amorphous with fine projections (variant XX), characteristic structures of the spikelets of *Oryza grandiglumis* (ICN MHN FIT 1062). **E**, bilobate short cell with short acute projections and concave ends (variant I) from *Oryza latifolia* leaf (ICN MHN FIT 1067). **F**, trapeziform with sinuate base with two acute projections (variant Y), from spikelets of *Oryza grandiglumis* (ICN MHN FIT1062). Codes in parenthesis refer to the accession numbers of the slide preparations in the Phytolith Collection of the *Instituto de Ciencias Naturales* (ICN, 2019).

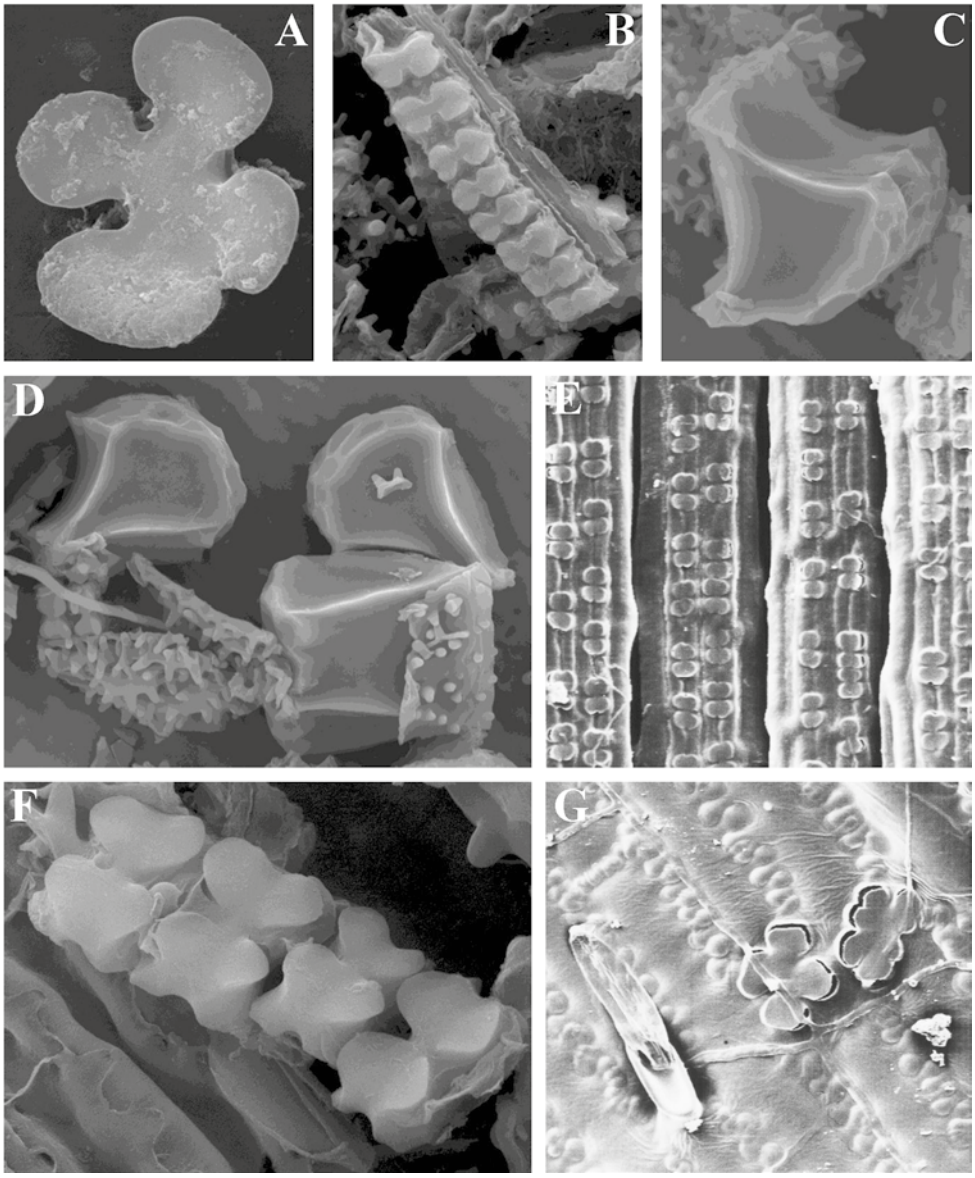

Figure 3. Phytoliths of Amazonian grasses (SEM). **A** and **G**, bilobate short cell. **B, E** and **F**, bilobate long cells. **C** and **D**, bulliform cells.

Cluster analyses and patterns at subfamily level. In both separate and combined UPGMA analyses, we failed to recover clusters that contained only members of a single subfamily, with the exception of Pharoideae, represented by only two species of *Pharus* in our sample. Tribal or subtribal relations are not reflected in the clusters either. Although 2/3 of the species in our dataset are Panicoideae, we expected to recover distinct Bambusoideae, Chloridoideae,

Oryzoideae and Aristidoideae clusters in either the combined (Fig. 4) or GSSCP only dataset (Fig. 5), but all four subfamilies were interspersed with the panicoids throughout both dendrograms. The GSSCP-only analysis was the one that gave results that most closely matched our hypothesis. In this dataset, Chloridoideae were concentrated in two clusters, although the largest of these was intermixed with two oryzoids and a panicoid, and numerous chloridoid species also fell outside of the two main clusters (Fig. 5), while within these clusters, genera did not group together, but were dispersed throughout the topology. In the same analysis, the two Pharidoideae did group together, although in the combined analysis, the panicoid *Digitaria fuscescens* also formed part of this cluster. Although the aristidoids in the Amazonian grass flora have characteristic bilobate long cell phytoliths with a very thin central shaft, all of the varieties of this morphotype category that we observed in Aristidoideae were also found in panicoid grasses in our sample, and thus they did not form a subfamily cluster. We explored the data further to see if the general Aristid morphotype (Neumann *et al.*, 2017) is associated with a particular habitat or photosynthetic pathway in the Amazonian panicoids (Table 2), but we found no relation. The bambusoids, also did not form a subfamily cluster because the distribution of the diagnostic variants (above) is at species or genus level. The same can be said for Oryzoideae. The UPGMA analysis of only the silicified epidermal structures (Fig. 6) was the least resolved, with many collapsed branches and the clusters not corresponding to subfamilies or lower taxonomic levels, with the exception of a few pairs of congeneric species.

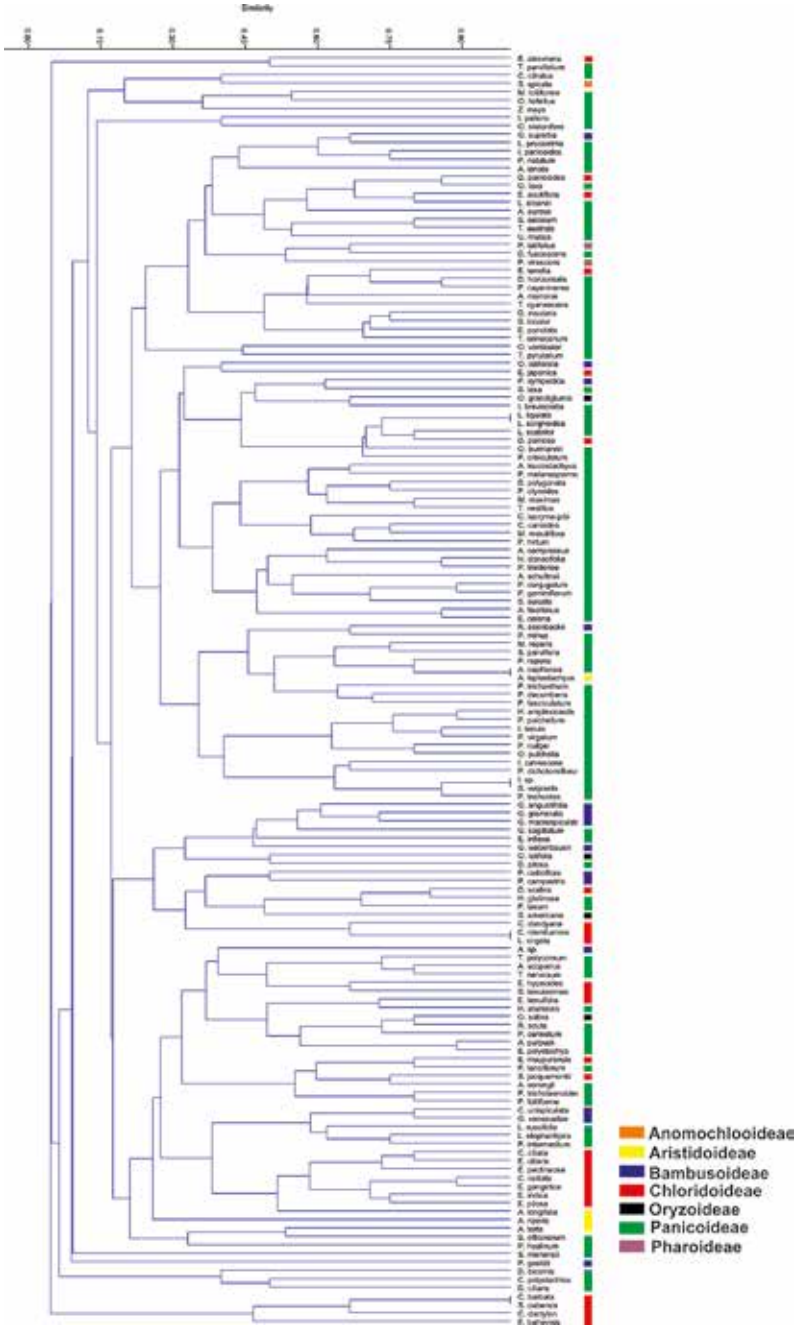

Figure 4. UPGMA analysis of combined matrix including all 54 phytolith variants: GSSCPs and silicified epidermal structures.<

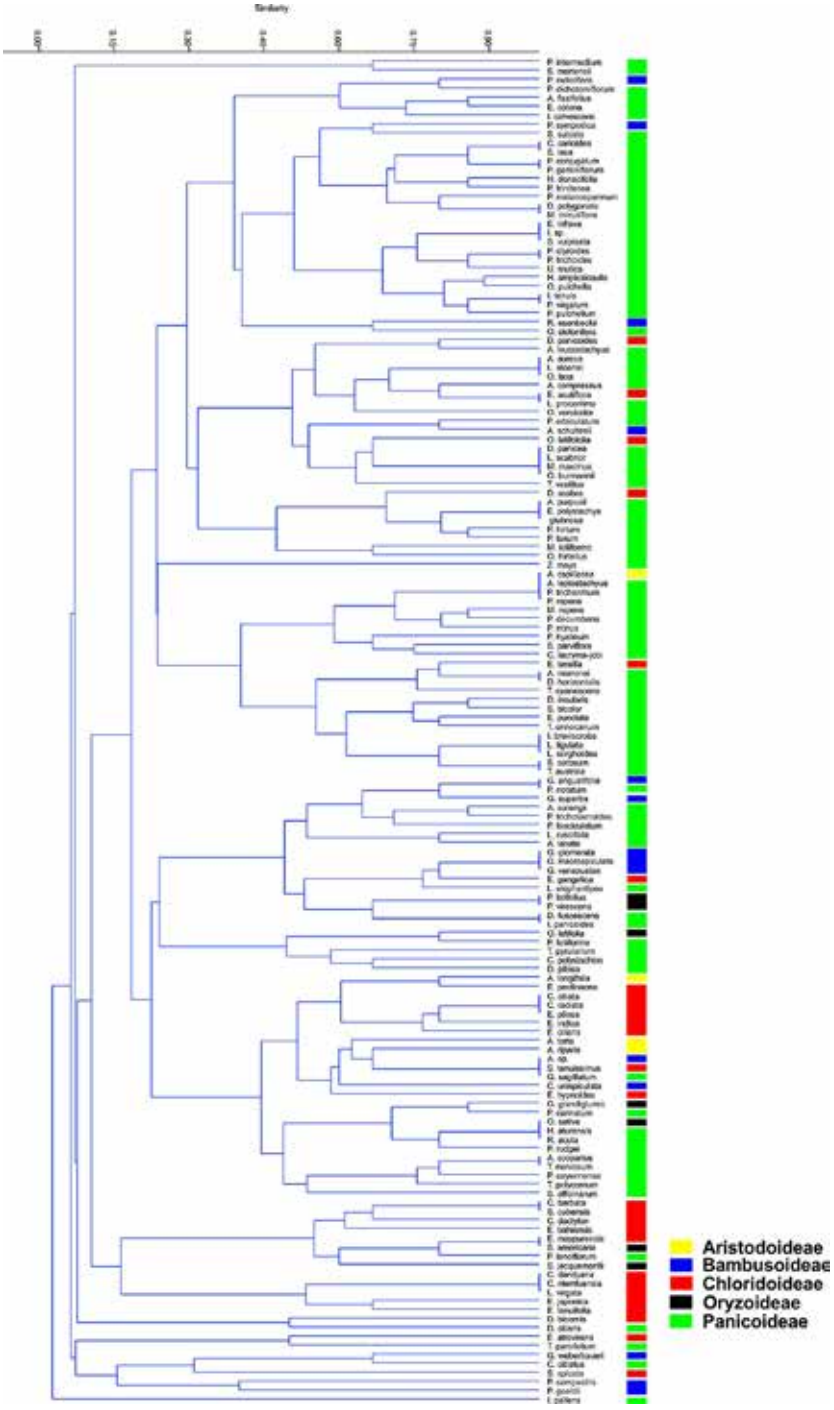

Figure 5. UPGMA analysis of matrix with 32 GSSCP variants.

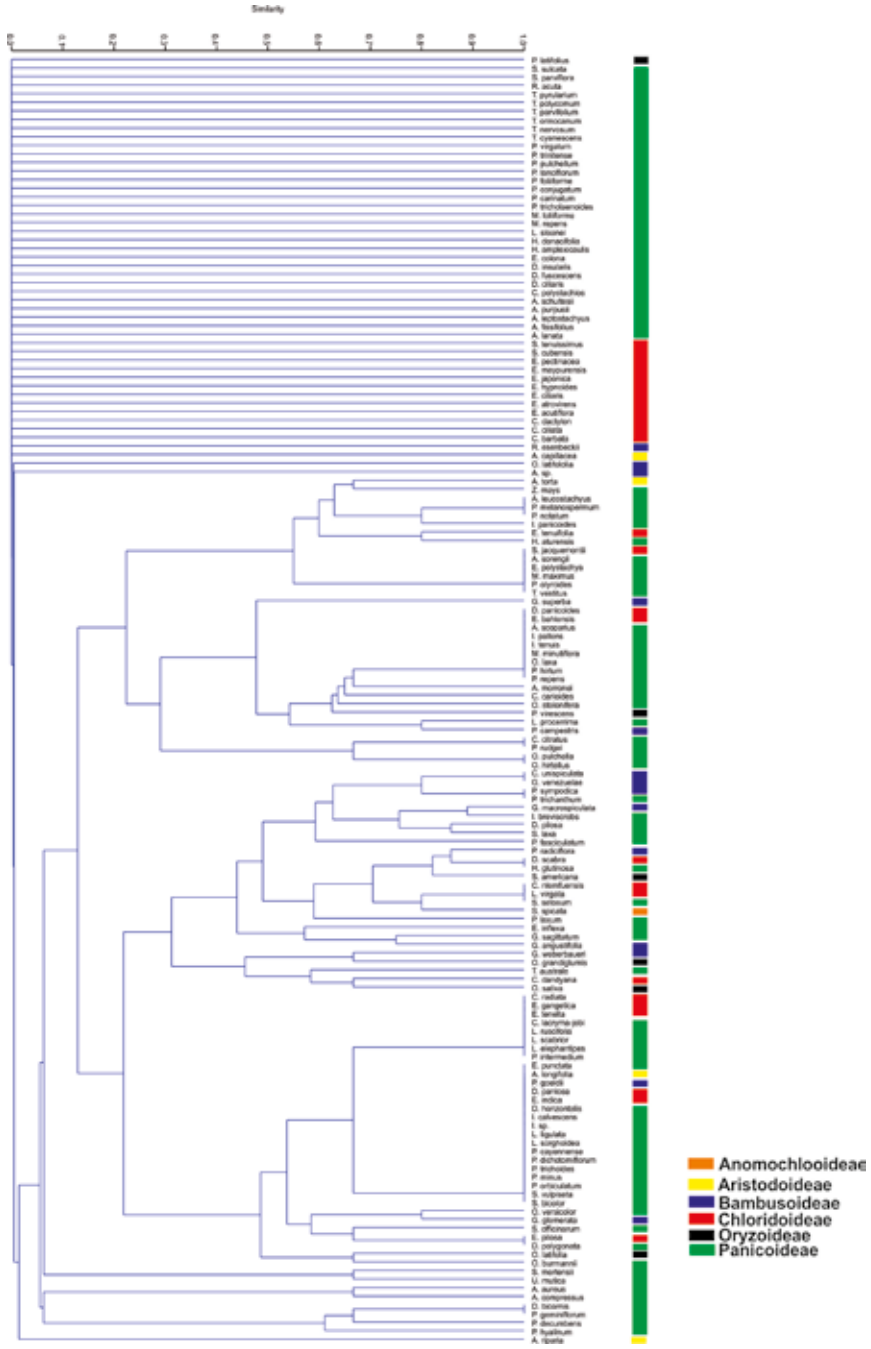

Figure 6. UPGMA analysis of matrix with 22 variants of (non GSSCP) silicified epidermal structures.

Discussion

Potential of non-GSSCP phytoliths. Phytolith research in grasses (reviewed in Piperno, 2006; Strömberg, 2018) has focused heavily on GSSCPs, but in our experience, silicified epidermal cells, stomata, prickles, and trichomes often appear in Amazonian archaeological contexts and here we have presented examples of silicified epidermal cells recovered from archaeological and paleoecological sediments that can be used to diagnose grasses to species level or at least greatly reduce the universe of possible taxa. Based on the fact that unique variants of epidermal cells were identified in several species in this study, we believe it is a promising area for future research, and given that some of these structures were found in culms and inflorescences, we concur with Piperno (2006) that it is worth expanding phytolith reference collections to include these organs. Bulliform cells are found only in grasses [although Albert Cristóbal (1995) erroneously stated that they also occur in other commelinid monocots], and they are highly variable in Amazonian species. Because of their function in responding to hydric stress, phytoliths derived from bulliform cells might be predicted to be more prevalent in C_4 grasses, but this is not the case; they are present in all lineages, in forest understory species as well as grasses of open areas (Table 2). We have detected additional variants in this phytolith category that remain to be described and their distribution documented. Overall, we conclude that silicified epidermal structures while not useful for diagnosing grass subfamilies, have potential as diagnostic markers at species level.

We must nevertheless acknowledge some limitations of this study. Because we do not know a lot about what drives silification of epidermal cells and hairs we cannot interpret their biological significance and we cannot be sure that presence of these structures in the taxa reported here will be consistent in all individuals of the same species, although the archaeological *Guadua angustifolia* example is encouraging. Strömberg (2016, 2018) suggests there may be some correlation with abundance of bulliform cells in sediments and high-light environments, but this hypothesis requires further testing, and it may be that for the Amazon region, this generality will not hold (see Tables 1 and 2; Fig. 2). For future studies it would be desireable to sample multiple populations of widespread species that live in both open and forested habitats to see how/if phytolith morphology and abundance change with environmental conditions.

In Table 1 we included the category "miscellaneous epidermal structures" which includes stomata and various types of hairs. We did not subdivide this category very finely, but future studies in this area could lead to finer taxonomic resolution, given that hairs are often important in diagnosing grass species. As a final comment on anatomical data, we note that orientation of GSSCPs in the leaf tissues was emphasized by Rudall *et al.* (2014) as being of taxonomic

importance, but orientation cannot be determined from phytoliths found free in sediments. Reference collections for archaeological and paleoecological studies are made from phytoliths extracted from calcinated leaf tissue, not from histological preparations and so contemporary phytolith collections lack this information, but our method does have the advantage of isolating silicified epidermal structures, which are less likely to be detected in histological preparations, as well as the advantage noted by Piperno (2006) of being able to see GSSCPs from multiple angles.

Taxonomic distribution of GSSCPs. While it is true that certain morphotypes have been identified as providing taxonomic resolution at the subfamily level, for example in chloridoid and pooid grasses (Brown, 1984; Piperno & Pearsall, 1998; Strömberg, 2016), it cannot be generalized that phytoliths are only or even most useful at this taxonomic level. Much in the way that chloroplast genes like *rbc*L and *mat*K were once used only in systematic studies at family level and above, we now know that autapomorphies in these genes can be useful diagnostic markers at species level. The same can be said for phytoliths. Broadening the sample both geographically and taxonomically is necessary to affirm or refute established patterns. As more studies are published, we expect to see more overlap of broad phytolith categories in multiple subfamilies, while variation at a finer scale becomes increasingly important (Piperno, 2006; Neumann *et al.*, 2017). Panicoideae is of particular importance in the lowland Neotropics: it is the only subfamily with both C_3 and C_4 photosynthesis and it also happens to be the most diverse subfamily in the Amazon. In our study we observed no clear pattern of morphotype distribution within the subfamily, with unique variants being restricted to one or few species (Table 1), a finding similar to that of Neumann *et al.* (2017) who surveyed a representative sample of West African grasses which also have a high proportion of panicoids, nevertheless they found less overlap of morphotypes among subfamilies, compared with our much larger Amazonian sample. The same authors also stressed that in West Africa, there is no clear relationship between GSCCP morphotypes and specific ecological conditions, a result echoed in our findings here.

Even when phytolith morphologies do not overlap between subfamilies, there is still need for caution in applying patterns too broadly. For example, Bambusoideae includes morphotypes found only in this subfamily, but there is no single variant that is distributed in all bambusoids. Piperno & Pearsall (1998) included a large number of species of the tribe Olyreae in their neotropical grass study, finding diagnostic phytoliths at subtribe and generic levels in this group, but lowland tropical species have other diagnostic morphologies (*Piresia*, *Pariana*, some *Guadua* species). We stress the importance of sampling, both at regional and taxonomic levels to better elucidate patterns of phytolith distribution within and among grass subfamilies.

Final considerations. We have confirmed unusual phytolith morphologies in some previously sampled taxa like *Pharus* and *Streptochaeta*, so even though we did not sample multiple individuals from different populations, congruence across these independent studies suggests that morphologies are consistent within individual species. We have also found additional structures not previously reported. It is therefore possible that in future studies, other authors who sample the same taxa reported here may find additional structures as well. We have not done counts to show relative abundance of different morphotypes within a given species and this is a worthwhile goal of future research, as is the SEM study of the morphotypes.

In this study we recognized 54 morphotype variants, which is not as high as in other studies: Neumann *et al.* (2017) recognized 153 variants in 54 species from 32 genera of African grasses, while Zucol (1998, 2000) found close to 50 variants each in samples of only eight species of *Panicum* and *Paspalum*. Subjectivity remains an outstanding issue, and we look forward to new developments in the use of pattern recognition software (T. Gallaher, pers. comm.) to compare how the specialist eye performs against machine learning algorithms. Finally, we would like to highlight that well-curated herbarium collections are an important source of material for phytolith reference collections. We also underscore the importance of collaboration with taxonomic specialists to ensure that material is properly determined and to aid in the interpretation of patterns of phytolith variation within large families.

Cited bibliography

Albert Cristóbal, R. 1995. Nuevo sistema de análisis descriptivo para fitolitos de sílice. *Pyrenae* 26: 19-38.

Ball, T. B., J. S. Gardner & N. Andreson. 1999. Identifying inflorescence phytoliths from selected species of wheat (*Triticum monococum*, *T. dicoccon*, *T. dicoccoides*, and *T. aestivum*) and Barley (*Hordeum vulgare* and *H. spontaneum*) (Gramineae). *American Journal of Botany* 86: 1615-1623. https://doi.org/10.2307/2656798

Bremond, L., A. Alexandre, M. Wooller, C. Hély, D. Williamson, P. Schäfer, A. Majule & J. Guiot. 2008. Phytolith indices as proxies of grass subfamilies on East African tropical mountains. *Global and Planetary Change* 61: 209-224. https://doi.org/10.1016/j.gloplacha.2007.08.016

Brown, D. A.1984. Prospects and limits of a phytolith key for grasses in the Central United States. *Journal of Archaeological Science* 11: 345-368. https://doi.org/10.1016/0305-4403(84)90016-5

Cavalcante, P. 1968. Contribuição ao estudo dos corpos silicosos das gramíneas amazônicas. *Boletim do Museu Paraense Emilio Goeldi (Botânica)* 30:1-38.

Ellis, R. 1979. A procedure for standardizing comparative leaf anatomy in the Poaceae. II. The epidermis as seen in surface view. *Bothalia* 12: 641-671. https://doi.org/10.4102/abc.v12i4.1441

Ferreira, M. J., C. Levis, J. Iriarte, C. R. Clement. 2019. Legacies of intensive management if forests around pre-Columbian and modern settlements in the Madeira-Tapajós interfluve, Amazonia. *Acta Botânica Brasilica* 33: 212-220. https://doi.org/10.1590/0102-33062018abb0339

Gallego, L. & R. A. Distel. 2004. Phytolith assemblages in grasses native to Central Argentina. *Annals of Botany* 94: 865-874. https://doi.org/10.1093/aob/mch214

Giraldo-Cañas D. 2013. Las gramíneas de Colombia. Riqueza, distribución, endemismo, invasión, migración, usos y taxonomías populares. Bogotá **D. C.**: Instituto de Ciencias Naturales, Universidad Nacional de Colombia.

Henry, A. G., P. S. Ungar, B. H. Passey, M. Sponheimer, L. Rossouw & M. Bamford. 2012. The diet of *Australopithecus sediba*. *Nature* 487: 90-93. https://doi.org/10.1038/nature11185

Hilbert, L. E. Góes Neves, F. Pugliense, B. Whitney, M. Shock, E. Veasey, C. Zimpel & J. Iriarte. 2017. Evidence for mid-Holoceno rice domestication in the Americas. *Nature Ecology & Evolution* 1: 1693-1698. https://doi.org/10.1038/s41559-017-0322-4

Hoorn, C. G. Bogotá, M. Romero-Báez, E. Lammertsma, S. Flantua, E. Dantas, R. Dino, D. Carmo, J. F. Chemale. 2017. The Amazon at sea: onset and stages of the Amazon river from a marine record, with special reference to Neogene plant turnover in the drainage basin. *Global*

Planet Change 153: 51-65. http://dx.doi.org/10.1016/j.gloplacha.2017.02.005

Hoorn, C., T. Kukla, G. Bogotá-Ángel, E. van Soelen, C. González-Arango, F. P. Wesselingh, H. Vonhof, P. Val, G. Morcote-Ríos, M. Roddaz, E. L. Dantas, R. Ventura Santos, J. S. Sinninghe Damsté, J.-H. Kim & R. J. Morley. 2022. Cyclic sediment deposition by orbital forcing in the Miocene wetland of western Amazonia? New insights from a multidisciplinary approach. Global and Planetary Change 210: 103717. https://doi.org/10.1016/j.gloplacha.2021.103717

Instituto de Ciencias Naturales (ICN). 2019. Colecciones en línea. http://www.biovirtual.unal.edu.co/fitolitos.

Khan, R., S. Z. Ul Abidin, A. S. Mumtaz, S. Jamsheed& H. Ullah. 2017. Comparative leaf and pollen micromorphology on some grass taxa (Poaceae) distributed in Pakistan. *International Journal of Nature and Life Sciences* 1: 72-82.

Londoño, X. & M. Kobayashi. 1991. Estudio comparativo entre los cuerpos silíceos de *Bambusa* y *Guadua*. *Caldasia* 16: 407-418.

Madella, M., A. Alexandre & T. Ball. 2005. International code of phytolith nomenclaure 1.0. *Annals of Botany* 96: 253-260. https://doi.org/10.1093/aob/mci172

McMichael, C. & M. Bush. 2019. Spaciotemporal patterns of the precolumbian people in Amazonia. *Quaternary Researech* 92: 53-69. https://doi.org/10.1017/qua.2018.152

Morcote-Ríos, G., D. Giraldo-Cañas & L. Raz. 2015. *Illustrated catalogue of contemporary phytoliths for archaeology and paleoecology. I. Amazonian grasses of Colombia*. Bogotá D. C.: Instituto de Ciencias Naturales, Universidad Nacional de Colombia.

Neumann, K., A. G. Fahmy, N. M**ü**ller-Scheeβel & M. Scmmidt. 2017. Taxonomic, ecological and paleoecological significance of leaf phytoliths in west African grasses. *Quaternary International* 434: 15-32. http://dx.doi.org/10.1016/j.quaint.2015.11.039

Palmer, P. G. & A. E. Tucker. 1981. A scanning electron microscope survey of the epidermis of East African grasses, I. Smithsonian Contributions to Botany 49: 1-84. https://doi.org/10.5479/si.0081024X.49

Pearsall, D. 1989. *Paleoethnobotany: A handbook of procedures.* San Diego: Academic Press.

Piperno, D. R.1988. *Phytolith analysis*. *An archaeological and geological perspective*. San Diego: Academic Press.

Piperno, D. R. 1997. Phytoliths and microscopic charcoal from leg 155: a vegetational and fire history of the Amazon basin during the last 75 K.Y. In: R. D. Flodd, D. J. W. Piper, A. Klaus & L. C. Peterson (eds.), *Proceedings of the Ocean Drilling Program, Scientific*

Results 155: 411-418. https://doi.org/10.2973/odp.proc.sr.155.250.1997

Piperno, D. R. 2006. *Phytoliths. A comprehensive guide for archaeologists and paleoecologists*. Lanham: Altamira Press.

Piperno, D. R. & D. M. Pearsall. 1998. *The silica bodies of tropical American grasses: morphology, taxonomy, and implications for grass systematic and fossil phytolith identification*. Washington, D.C.: Smithsonian Institution Press.

Prat, H. 1932. L'épiderme des graminées. Étude anatomique et systématique. *Annales des Sciences Naturelles: Botanique (sér. 10)* 14: 117-324.

Prychid, C., P. Rudall & M. Gregory. 2003. Systematics and biology of silica in monocotyledons. *The Botanical Review* 69: 377-440. https://doi.org/10.1663/0006-8101(2004)069[0377:SABOSB]2.0.CO;2

Richards, P. W. 1996. *The tropical rain forest and ecological study*. Second edition. Cambridge: Cambridge University Press.

Rudall, P. J., C. Prychid & T. Gregory T. 2014. Epidermal patterning and silica phytoliths in grasses: An evolutionary history. *The Botanical Review* 80: 59-71. https://doi.org/10.1007/s12229-014-9133-3

Soreng, R. J., P. M. Peterson, K. Romaschenko, G. Davidse, J. K. Teisher, L. G. Clark, P. Barberá, L. J. Gillespie & F. O. Zuloaga. 2017. A worldwide phylogenetic classification of the Poaceae (Gramineae) II: An update and a comparison of two 2015 classifications. *Journal of Systematics and Evolution* 55: 259-290. https://doi.org/10.1111/jse.12262

Strömberg, C. A. E. 2006. The evolution of hypsodonty in equids: testing a hypothesis of adaptation. *Paleobiology* 32: 236-258. https://doi.org/10.1666/0094-8373(2006)32[236:eohiet]2.0.co;2

Strömberg, C. A. E., R. Dunn, C. Crifò & E. Harris. 2018. Phytoliths in paleoecology: analytical considerations, current use, and future directions. In: D. Croft, D. Su & S. Simpson (eds.), *Methods in Paleoecology: reconstructing Cenozoic terrestrial environments*: 235-287. Cham: Springer.

Strömberg, C. A. E., V. S. Di Stilio & Z. Song. 2016. Functions of phytoliths in vascular plants: an evolutionary perspective. *Functional Ecology* 30: 1286-1297. https://doi.org/10.1111/1365-2435.12692

Twiss, P. C, E. Suess & R. M. Smith. 1969. Morphological classification of grass phytoliths. *Soil Science Society of America Proceeding* 33: 109-115. https://doi.org/10.2136/sssaj1969.03615995003300010030x

Whang, S., K. Kim & W. Hess. 1998. Variation of silica bodies in leaf epidermal long cell within and among seventeen species of *Oryza* (Poaceae). *American Journal of Botany* 85: 461-466. https://doi.org/10.2307/2446428

Zhao, Z. J., D. M. Pearsall, R. A. Benfer & D. R. Piperno. 1998. Distinguishing rice (*Oriza sativa* Poaceae) from wild *Oryza* species throung phytolith analysis. II: Finalized method. *Economic Botany* 52: 134-145.

Zucol, A. 1992. Microfitolitos: I. Antecedentes y terminología. *Ameghiniana* 29: 353-362.

Zucol, A. 1998. Microfitolitos de las Poaceae argentinas: II. Microfitolitos foliares de algunas especies del género *Panicum* (Poaceae, Paniceae) de la provincia de Entre Ríos. *Darwiniana* 36: 29-50.

Zucol, A. 2000. Fitolitos de Poaceae de Argentina. III. Fitolitos foliares de especies del género *Paspalum* (Paniceae) en la provincia de Entre Ríos. *Darwiniana* 38: 11-32.

Acknowledgements

We thank Carina Hoorn (Institute for Biodiversity and Ecosystem Dynamics, University of Amsterdam, The Netherlands) for sharing her Miocene sediment samples with us, Cristian Pinzón (*Instituto de Ecología*, Xalapa, Mexico) for assistance with the cluster analyses, and *Universidad Nacional de Colombia*. We thank the reviewers (Prof. Dr. Orlando Rangel and Prof. Dr. Alexis Jaramillo-Justinico) and editors for their valuable comments on the manuscript.

Conflicts of interest. The authors declare none conflicts of interest in the publication.

Table 1. Distribution of phytolith morphotypes in species of Amazonian grasses (*see Fig. 1 YY-ZZ).

Taxon	Bilobate Short Cell	Bilobate Long Cell	Polylobate	Trapeziform	Cross	Suborbicular-Rectangular	Carinate	Bulliform Cell	Elongate Epidermal Cell	Amorphous with Projections	Misc. Epidermal Structures*	Mammiform-Conical Cell	
Anomochlooideae													
Streptochaeta spicata Schrad. ex Nees		N	O	S-T			EE	HH-II	RR				
Aristidoideae													
Aristida capillacea Lam.	D	L	P										
Aristida longifolia Trin.		L		U					PP				
Aristida riparia Trin.		J		U					OO-QQ				
Aristida torta (Nees) Kunth		M		U					OO-RR		YY-ZZ		
Bambusoideae													
Arthrostylidium sp.				U				FF				AAA	
Cryptochloa unispiculata Soderstr.				R-U				HH	PP		ZZ		
Guadua angustifolia Kunth	A			U				HH	PP	WW	YY		
Guadua glomerata Munro	A			U				II	PP		YY		
Guadua macrospiculata Londoño & L.G. Clark	A			U				HH-II	PP		YY		
Guadua superba Huber	A-G			W				JJ-KK			ZZ		
Guadua venezuelae Munro	A			U				HH	PP		ZZ		
Guadua weberbaueri Pilg.	A			S				II			YY		

Taxon	Bilobate Short Cell	Bilobate Long Cell	Polylobate	Trapeziform	Cross	Suborbicular-Rectangular	Carinate	Bulliform Cell	Elongate Epidermal Cell	Amorphous with Projections	Misc. Epidermal Structures*	Mammiform-Conical Cell	
Olyra latifololia L.	B			T				GG					
Pariana campestris Aubl.	A			T-V				HH			ZZ		
Pariana radiciflora Sagot ex Döll			P	V-W				GG-HH-II			ZZ		
Piresia goeldii Swallen				T	Z				PP				
Piresia sympodica (Döll) Swallen	B-C-G		P	T				HH	PP				
Raddiella esenbeckii (Steud.) Calderón & Soderstr.	C		O-P	U									
Chloridoideae													
Chloris barbata Sw.						BB							
Chloris ciliata Sw.				U		BB							
Chloris dandyana C.D. Adams						BB		II-JJ					
Chloris radiata (L.) Sw.				U		BB			PP		ZZ		
Cynodon dactylon (L.) Pers.						BB-CC							
Cynodon nlemfuensis Vanderyst						BB		HH-II					
Dinebra panicea (Retz.) P. M. Peterson & N. Snow	B								PP				
Dinebra panicoides (J. Presl) P. M. Peterson & N. Snow	A-B	K									ZZ		
Dinebra scabra (Nees) P. M. Peterson & N. Snow	B-H							HH-II			ZZ		
Eleusine indica (L.) Gaertn.	G			U		BB			PP				

Taxon	Bilobate Short Cell	Bilobate Long Cell	Polylobate	Trapeziform	Cross	Suborbicular-Rectangular	Carinate	Bulliform Cell	Elongate Epidermal Cell	Amorphous with Projections	Misc. Epidermal Structures*	Mammiform-Conical Cell	
Eragrostis acutiflora (Kunth) Nees	A-B			W									
Eragrostis atrovirens (Desf.) Trin. ex Steud.	B			W							ZZ		
Eragrostis bahiensis Schrad. ex Schult.		J				CC					ZZ		
Eragrostis ciliaris (L.) R. Br.	C			U		BB							
Eragrostis gangetica (Roxb.) Steud.	A			U		BB			PP		ZZ		
Eragrostis hypnoides (Lam.) Britton, Stern & Poggenb.				U		AA							
Eragrostis japonica (Thunb.) Trin.	B					BB							
Eragrostis maypurensis (Kunth) Steud.				U		CC							
Eragrostis pectinacea (Michx.) Nees		L		U		BB							
Eragrostis pilosa (L.) P. Beauv.				U		BB			PP		YY		
Eragrostis tenella (L.) P. Beauv. ex Roem. & Schult.	A-D					CC			PP		ZZ		
Eragrostis tenuifolia (A. Rich.) Hochst. ex Steud.	B			U		BB-CC			SS		YY		
Leptochloa virgata (L.) P. Beauv.						BB		HH-II					

Taxon	Bilobate Short Cell	Bilobate Long Cell	Polylobate	Trapeziform	Cross	Suborbicular-Rectangular	Carinate	Bulliform Cell	Elongate Epidermal Cell	Amorphous with Projections	Misc. Epidermal Structures*	Mammiform-Conical Cell	
Sporobolus cubensis Hitchc.						CC							
Sporobolus jacquemontii Kunth				W		CC					YY		
Sporobolus tenuissimus (Mart. ex Schrank) Kuntze				W		CC							
Oryzoideae													
Oryza grandiglumis (Döll) Prod.	B			U-Y				II	PP	XX	YY		
Oryza latifolia Desv.	I			U-W				II	PP-RR-TT				
Oryza sativa L.	B			U				II					
Streptogyna americana C.E. Hubb.				U		CC		HH-II-LL			ZZ		
Panicoideae													
Andropogon leucostachyus Kunth	B	K									YY-ZZ		
Anthaenantia lanata (Kunth) Benth.	A	J		W									
Arthropogon sorengii Gir.-Cañas	A			U-W		CC					YY		
Axonopus aureus P. Beauv.	A-B							HH	NN				
Axonopus compressus (Sw.) P. Beauv.	B			W					NN				
Axonopus fissifolius (Raddi) Kuhlm.		K	P	W									
Axonopus leptostachyus (Flüggé) Hitchc.	D		P										

Taxon	Bilobate Short Cell	Bilobate Long Cell	Polylobate	Trapeziform	Cross	Suborbicular-Rectangular	Carinate	Bulliform Cell	Elongate Epidermal Cell	Amorphous with Projections	Misc. Epidermal Structures*	Mammiform-Conical Cell	
Axonopus morronei Gir.-Cañas	A-D								QQ		ZZ		
Axonopus purpusii (Mez) Chase	B-G-H			U									
Axonopus schultesii G. A. Black	B		P	S									
Axonopus scoparius (Flüggé) Kuhlm.	D			U							ZZ		
Cenchrus polystachios (L). Morrone	B	J-K-M	P	W									
Coix lacryma-jobi L.	B-D	L	P						PP		ZZ		
Coleataenia carioides (Nees ex Trin.) Soreng	B		P	U							ZZ	AAA	
Cymbopogon citratus (DC.) Stapf				S					RR				
Dallwatsonia pilosa (Sw.) J. R. Grande	B-C			U-W				HH-II	PP-SS				
Dallwatsonia polygonata (Schrad.) J. R. Grande	B		P						PP		YY		
Digitaria bicornis (Lam.) Roem. & Schult.		M	P						SS				
Digitaria ciliaris (Retz.) Koeler		J-M											
Digitaria fuscescens (J. Presl) Henrard	A		P						PP				
Digitaria horizontalis Willd.	A-D								PP				
Digitaria insularis (L.) Fedde	A-D			W									
Echinochloa colona (L.) Link		K	O-P	W									

Taxon	Bilobate Short Cell	Bilobate Long Cell	Polylobate	Trapeziform	Cross	Suborbicular-Rectangular	Carinate	Bulliform Cell	Elongate Epidermal Cell	Amorphous with Projections	Misc. Epidermal Structures*	Mammiform-Conical Cell	
Echinochloa polystachya (Kunth) Hitchc.	B-G-H			U							YY		
Echinolaena inflexa (Poir.) Chase	A		P					HH	TT		YY		
Eriochloa punctata (L.) Desv. ex Ham.	D			W					PP				
Gynerium sagittatum (Aubl.) P. Beauv.				U		AA		HH-II			YY		
Homolepis aturensis (Kunth) Chase	B			U					SS		YY-ZZ		
Homolepis glutinosa (Sw.) Zuloaga & Soderstr.	B-G-H			U				HH-II			ZZ		
Hymenachne amplexicaulis (Rudge) Nees	A-B		P	S-U									
Hymenachne donacifolia (Raddi) Chase	B		P	W									
Ichnanthus breviscrobs Döll	B-D							HH-II	OO-PP		YY		
Ichnanthus calvescens (Nees ex Trin.) Döll		K	P						PP				
Ichnanthus pallens(Sw.) Munro ex Benth.		K		R							ZZ		
Ichnanthus panicoides P. Beauv.	A							KK			YY-ZZ		
Ichnanthus tenuis (J. Presl & C. Presl) Hitchc. & Chase	A		P	U							ZZ		

Taxon	Bilobate Short Cell	Bilobate Long Cell	Polylobate	Trapeziform	Cross	Suborbicular-Rectangular	Carinate	Bulliform Cell	Elongate Epidermal Cell	Amorphous with Projections	Misc. Epidermal Structures*	Mammiform-Conical Cell	
Ichnanthus sp.	A		P						PP				
Lasiacis ligulata Hitchc. & Chase	B-D								PP				
Lasiacis procerrima (Hack.) Hitchc.	A-B			W				HH-KK			ZZ		
Lasiacis ruscifolia (Kunth) Hitchc.	A	J							PP		ZZ		
Lasiacis scabrior Hitchc.	B								PP		ZZ		
Lasiacis sloanei (Griseb.) Hitchc.	A-B												
Lasiacis sorghoidea (Desv. ex Ham.) Hitchc. & Chase	B-D								PP				
Louisiella elephantipes (Nees ex Trin.) Zuloaga	A-C			U					PP		ZZ		
Megathyrsus maximus (Jacq.) B.K Simon & S.W.L. Jacobs	B										YY		
Melinis minutiflora P. Beauv.	B		P								ZZ		
Melinis repens (Willd.) Zizka	D	L	P	U									
Mesosetum loliiforme (Hochst. ex Steud.) Chase	G-H			S-W									
Ocellochloa pulchella (Raddi) Zuloaga & Morrone	A-B-E		P	U					RR		ZZ		
Ocellochloa stolonifera (Poir.) Zuloaga & Morrone		K	O-P	U			EE	MM			ZZ		

Taxon	Bilobate Short Cell	Bilobate Long Cell	Polylobate	Trapeziform	Cross	Suborbicular-Rectangular	Carinate	Bulliform Cell	Elongate Epidermal Cell	Amorphous with Projections	Misc. Epidermal Structures*	Mammiform-Conical Cell	
Oplismenus burmannii (Retz.) P. Beauv.	B								PP-RR				
Oplismenus hirtellus (L.) P. Beauv.	A-G-H		P	W					RR		ZZ		
Orthoclada laxa (Rich.) P. Beauv.	A-B										ZZ		
Otachyrium versicolor (Döll) Henrard	A-B			S-W			EE	JJ	PP				
Panicum cayennense Lam	A-D			U					PP				
Panicum dichotomiflorum Michx			P	W					PP				
Panicum hirtum Lam	B-G-H		P								ZZ		
Panicum olyroides Kunth	A-B		P								YY		
Panicum rudgei Roem. & Schult.	A-B			U					RR				
Panicum trichanthum Nees	D		P					HH	PP				
Panicum trichoides Sw.	A-B		P						PP				
Panicum tricholaenoides Steud.	A			U-W									
Paspalum carinatum Humb. & Bonpl. ex Flüggé	B-D			U									
Paspalum conjugatum P.J. Bergius	B	K	P	U									
Paspalum decumbens Sw.	D		P	U				HH	SS				
Paspalum fasciculatum Willd. ex Flüggé	A-D		P	U-W				HH	PP-SS-VV				

Taxon	Bilobate Short Cell	Bilobate Long Cell	Polylobate	Trapeziform	Cross	Suborbicular-Rectangular	Carinate	Bulliform Cell	Elongate Epidermal Cell	Amorphous with Projections	Misc. Epidermal Structures*	Mammiform-Conical Cell	
Paspalum foliiforme S. Denham				U-W									
Paspalum geminiflorum Steud.	B	K	P	U					SS				
Paspalum hyalinum Nees ex Trin.	D	L							RR-SS				
Paspalum intermedium Munro ex Morong & Britton	C								PP		ZZ		
Paspalum lanciflorum Trin.				U-W		CC							
Paspalum laxum Lam.	B-G-H							HH-II-MM	QQ				
Paspalum melanospermum Desv. ex Poir.	B-E		P								YY-ZZ		
Paspalum minus E. Fourn.	C-D		P	U					PP				
Paspalum notatum Flüggé	A			W							ZZ		
Paspalum orbiculatum Poir.	B			S					PP				
Paspalum pulchellum Kunth	A		P	S-U									
Paspalum repens P.J. Bergius	D		P								ZZ		
Paspalum trinitense (Mez) S. Denham	B		P	U-W									
Paspalum virgatum L.	A		P	U									
Trichanthecium cyanescens (Nees ex Trin.) Zuloaga & Morrone	A-D		Q										
Trichanthecium nervosum (Lam.)	D			U									

Taxon	Bilobate Short Cell	Bilobate Long Cell	Polylobate	Trapeziform	Cross	Suborbicular-Rectangular	Carinate	Bulliform Cell	Elongate Epidermal Cell	Amorphous with Projections	Misc. Epidermal Structures*	Mammiform-Conical Cell	
Trichanthecium orinocanum (Luces) Zuloaga & Morrone	B-D			W									
Trichanthecium parvifolium (Lam.) Zuloaga & Morrone	A-F			X									
Trichanthecium polycomum (Trin.) Zuloaga & Morrone	D-G			U			EE						
Trichanthecium pyrularium (Hitchc. & Chase) Zuloaga & Morrone	G			W			EE						
Reimarochloa acuta (Flüggé) Hitchc.	B			U									
Saccharum officinarum L.	D	L-M		U-W					PP-RR-UU		YY		
Setaria parviflora (Poir.) Kerguélen	D	L	P	W									
Setaria sulcata Raddi	B-C	K	P										
Setaria vulpiseta (Lam) Roem. & Schult.	A		P						PP				
Sorghastrum setosum (Griseb.) Hitchc.	A-B-D												
Sorghum bicolor (L.) Moench.	A-B-D			W					PP				
Steinchisma laxa (Sw.) Zuloaga	B												
Stephostachys mertensii (Roth) Zuloaga & Morrone	C-D										YY		

Taxon	Bilobate Short Cell	Bilobate Long Cell	Polylobate	Trapeziform	Cross	Suborbicular-Rectangular	Carinate	Bulliform Cell	Elongate Epidermal Cell	Amorphous with Projections	Misc. Epidermal Structures*	Mammiform-Conical Cell	
Trachypogon vestitus Andersson	B-C										YY		
Tripsacum australe H.C. Cutler & E.S. Anderson	A-B-D							II	VV				
Urochloa mutica (Forssk.) T.Q. Nguyen	A-B-C		P					II-KK					
Zea mays L.	A-C-D-F-G-H	J	P-Q	S-U		AA-BB-CC		KK	RR-SS		YY-ZZ		
Pharoideae													
Pharus latifolius L.	A					DD							
Pharus virescens Döll	A					DD			TT		ZZ		

Table 2. Habitat and photosynthetic pathways of Amazonian grasses, adapted from Giraldo-Cañas (2013) and Morcote-Ríos *et al.* (2015). Subfamily species distribution as Table 1.

Taxon	Habitat	Photosynthetic Pathway
Streptochaeta spicata Schrad. ex Nees	Understory of mature humid lowland forests	C_3
Aristida capillacea Lam.	Savanas, slopes, rock out crops, grasslands	C_4
Aristida longifolia Trin.	Savannas	C_3
Aristida riparia Trin.	Savannas	C_4
Aristida torta (Nees) Kunth	Savannas	C_4
Arthrostylidium sp.	Forest edges	C_3
Cryptochloa unispiculata Soderstr.	Forest understory and forest edge	C_3
Guadua angustifolia Kunth	Secondary forest, riparian environments	C_3
Guadua glomerata Munro	Secondary forest, riparian environments	C_3
Guadua macrospiculata Londono & L.G. Clark	Secondary forest, riparian environments	C_3
Guadua superba Huber	Secondary forest, riparian environments	C_3
Guadua venezuelae Munro	Forest and riparian environments	C_3
Guadua weberbaueri Pilg.	Forest and riparian environments	C_3
Olyra latifololia L.	Forest edges	C_3
Pariana campestris Aubl.	Understory and forest edges	C_3
Pariana radiciflora Sagot ex Döll	Understory and forest edges	C_3
Piresia goeldii Swallen	Humid forest understory	C_3
Piresia sympodica (Döll) Swallen	Understory and forest edges	C_3
Raddiella esenbeckii (Steud.) Calderón & Soderstr.	Open areas with rocky or sandy substrates	C_3
Chloris barbata Sw.	Disturbed open areas	C_4
Chloris ciliata Sw.	Disturbed open areas	C_4
Chloris dandyana C.D. Adams	Disturbed open areas	C_4
Chloris radiata (L.) Sw.	Disturbed open areas	C_4
Cynodon dactylon (L.) Pers.	Disturbed open areas	C_4
Cynodon nlemfuensis Vanderyst	Disturbed open areas, roadsides	C_4
Dinebra panicea (Retz.) P. M. Peterson & N. Snow	Disturbed open areas	C_4

Taxon	Habitat	Photosynthetic Pathway
Dinebra panicoides (J. Presl) P. M. Peterson & N. Snow	Disturbed open areas	C_4
Dinebra scabra (Nees) P. M. Peterson & N. Snow	Disturbed open areas	C_4
Eleusine indica (L.) Gaertn.	Disturbed open areas, crops fields, roadsides	C_4
Eragrostis acutiflora (Kunth) Nees	Savannas, *"herbazales"* (areas dominated by herbaceous, non gramonoid vegetation), roadsides, disturbed open areas	C_4
Eragrostis atrovirens (Desf.) Trin. ex Steud.	Disturbed open areas	C_4
Eragrostis bahiensis Schrad. ex Schult.	Disturbed open areas	C_4
Eragrostis ciliaris (L.) R. Br.	Open field, disturbed open areas, roadsides, abandoned clearings	C_4
Eragrostis gangetica (Roxb.) Steud.	Disturbed open areas	C_4
Eragrostis hypnoides (Lam.) Britton, Stern & Poggenb.	Open areas, wet, sandy substrates, river and stream banks, lakeshores	C_4
Eragrostis japonica (Thunb.) Trin.	Disturbed open areas, open fields	C_4
Eragrostis maypurensis (Kunth) Steud.	Savannas, *"herbazales"* (areas dominated by herbaceous, non-graminoid vegetation) disturbed open areas, roadsides	C_4
Eragrostis pectinacea (Michx.) Nees	Savannas , *"herbazales"* (areas dominated by herbaceous, non-graminoid vegetation), disturbed open, roadsides	C_4
Eragrostis pilosa (L.) P. Beauv.	Disturbed open areas, abandoned clearings with low-statured vegetation	C_4
Eragrostis tenella (L.) P. Beauv. ex Roem. & Schult.	Disturbed open areas, roadsides, abandoned clearings	C_4
Eragrostis tenuifolia (A. Rich.) Hochst. ex Steud.	Disturbed open areas, roadsides, abandoned clearings with low-statured vegetation, open fields	C_4
Leptochloa virgata (L.) P. Beauv.	Disturbed open areas	C_4
Sporobolus cubensis Hitchc.	Savannas	C_4
Sporobolus jacquemontii Kunth	Disturbed open areas, savannas, roadsides	C_4
Sporobolus tenuissimus (Mart. ex Schrank) Kuntze	Disturbed open areas, roadsides	C_4

Taxon	Habitat	Photosynthetic Pathway
Oryza grandiglumis (Döll) Prod.	Marshy environments, swamps, wet fields, ditches and banks of ponds and small streams	C_3
Oryza latifolia Desv.	Marshy environments, swamps, wet fields, ditches and banks of ponds and small streams	C_3
Oryza sativa L.	Lowland and mid elevations in open vegetation on very wet or saturated soils	C_3
Streptogyna americana C.E. Hubb.	Humid forest understory	C_3
Andropogon leucostachyus Kunth	Savannas, disturbed open areas	C_4
Anthaenantia lanata (Kunth) Benth.	Savannas, *"herbazales"* (areas dominated by herbaceous, non-graminoid vegetation), rock outcrops, disturbed open areas	C_4
Arthropogon sorengii Gir.-Cañas	Savannas and *"herbazales"* (areas dominated by herbaceous, non-graminoid vegetation) associated with rock outcrops	C_4
Axonopus aureus P. Beauv.	Savannas, disturbed open areas	C_4
Axonopus compressus (Sw.) P. Beauv.	Savannas, disturbed open areas	C_4
Axonopus fissifolius (Raddi) Kuhlm.	Savannas, disturbed open areas	C_4
Axonopus leptostachyus (Flüggé) Hitchc.	Savannas, *"herbazales"* (areas dominated by herbaceous, non-graminoid vegetation), rock outcrops	C_4
Axonopus morronei Gir.-Cañas	Savannas	C_4
Axonopus purpusii (Mez) Chase	Savannas, disturbed open areas	C_4
Axonopus schultesii G. A. Black	Savanna, *"herbazales"* (areas dominated by herbaceous, non-graminoid vegetation), rock outcrops	C_4
Axonopus scoparius (Flüggé) Kuhlm.	Disturbed open areas, open fields	C_4
Cenchrus polystachios (L). Morrone	Disturbed open areas, open areas	C_4
Coix lacryma-jobi L.	Crops, open riparian areas	C_4
Coleataenia carioides (Nees ex Trin.) Soreng	Savannas, *"herbazales"* (areas dominated by herbaceous, non-gramonoid vegetation), rock outcrops	C_4
Cymbopogon citratus (DC.) Stapf	Cultivated in open areas	C_4

Taxon	Habitat	Photosynthetic Pathway
Dallwatsonia pilosa (Sw.) J. R. Grande	Savannas, disturbed open areas, roadsides, pastures, forest clearings	C_3
Dallwatsonia polygonata (Schrad.) J. R. Grande	Disturbed open areas, roadsides, banks of rivers and streams	C_3
Digitaria bicornis (Lam.) Roem. & Schult.	Savannas, disturbed open areas	C_4
Digitaria ciliaris (Retz.) Koeler	Savannas, disturbed open areas	C_4
Digitaria fuscescens (J. Presl) Henrard	Disturbed open areas	C_4
Digitaria horizontalis Willd.	Disturbed open areas, savannas, rock outcrops	C_4
Digitaria insularis (L.) Fedde	Disturbed open areas	C_4
Echinochloa colona (L.) Link	Disturbed open areas	C_4
Echinochloa polystachya (Kunth) Hitchc.	Back of rivers, lakes and swamps	C_4
Echinolaena inflexa (Poir.) Chase	Savannas, open areas	C_4
Eriochloa punctata (L.) Desv. ex Ham.	Forest edges, riverbanks	C_4
Gynerium sagittatum (Aubl.) P. Beauv.	Open rocky, stream and riverbanks	C_3
Homolepis aturensis (Kunth) Chase	Savannas, wet open areas, scrublands	C_3
Homolepis glutinosa (Sw.) Zuloaga & Soderstr.	Forest edges and open areas	C_3
Hymenachne amplexicaulis (Rudge) Nees	Banks of rivers, lakes and swamps	C_3
Hymenachne donacifolia (Raddi) Chase	Banks of rivers, lakes and swamps	C_3
Ichnanthus breviscrobs Döll	Edges and interior of humid forests	C_3
Ichnanthus calvescens (Nees ex Trin.) Döll	Edges and interior of humid forests	C_3
Ichnanthus pallens(Sw.) Munro ex Benth.	Edges and interior of humid forests	C_3
Ichnanthus panicoides P. Beauv.	Edges and interior of humid forests	C_3
Ichnanthus tenuis (J. Presl & C. Presl) Hitchc. & Chase	Edges and interior of humid forests	C_3
Ichnanthus sp.	Edges and interior of humid forests	C_3
Lasiacis ligulata Hitchc. & Chase	Edges of humid forest	C_3

Taxon	Habitat	Photosynthetic Pathway
Lasiacis procerrima (Hack.) Hitchc.	Disturbed open areas, secondary vegetation, open fields, roadsides	C_3
Lasiacis ruscifolia (Kunth) Hitchc.	Edges and interior of humid forests, secundary vegetation	C_3
Lasiacis scabrior Hitchc.	Edges of humid forest, secondary vegetation	C_3
Lasiacis sloanei (Griseb.) Hitchc.	Edges of humid forest, secondary vegetation	C_3
Lasiacis sorghoidea (Desv. ex Ham.) Hitchc. & Chase	Edges of humid forest, secondary vegetation	C_3
Louisiella elephantipes (Nees ex Trin.) Zuloaga	Banks of rivers, lakes and swamps	C_4
Megathyrsus maximus (Jacq.) B.K Simon & S.W.L. Jacobs	Disturbed open areas, roadsides, pastures, abandoned clearings with low-statured vegetation	C_4
Melinis minutiflora P. Beauv.	Disturbed open areas	C_4
Melinis repens (Willd.) Zizka	Disturbed open areas	C_4
Mesosetum loliiforme (Hochst. ex Steud.) Chase	Savannas and *"herbazales"* (areas dominated by herbaceous, non-graminoid vegetation)	C_4
Ocellochloa pulchella (Raddi) Zuloaga & Morrone	Forest edges, coffee plantations, roadsides	C_3
Ocellochloa stolonifera (Poir.) Zuloaga & Morrone	Sandy, humid areas, forest edges, banks of rivers and streams	C_3
Oplismenus burmannii (Retz.) P. Beauv.	Disturbed open areas and fields with light shade, open woods	C_3
Oplismenus hirtellus (L.) P. Beauv.	Disturbed open areas and fields with light shade, open woods	C_3
Orthoclada laxa (Rich.) P. Beauv.	Understory of humid forests, forest edges, cacao plantations	C_3
Otachyrium versicolor (Döll) Henrard	Savannas, *"herbazales"* (areas dominated by herbaceous, non-graminoid vegetation), rock outcrops	C_4
Panicum cayennense Lam.	Savannas, disturbed open areas	C_4
Panicum dichotomiflorum Michx.	Banks of rivers, lakes and swamps	C_4
Panicum hirtum Lam.	In forest clearings, forest edges, river banks	C_3
Panicum olyroides Kunth	Savannas, *"herbazales"* (areas dominated by herbaceous, non-graminoid vegetation), rock outcrops	C_4

Taxon	Habitat	Photosynthetic Pathway
Panicum rudgei Roem. & Schult.	Savannas, disturbed open areas	C_4
Panicum trichanthum Nees	In wet open areas, banks of rivers, lakes and swamps	C_3
Panicum trichoides Sw.	In wet open areas, shady areas, understory of humid forest, forest edges	C_3
Panicum tricholaenoides Steud.	Banks of rivers, lakes and swamps	C_4
Paspalum carinatum Humb. & Bonpl. ex Flüggé	Savannas , *"herbazales"* (areas dominated by herbaceous, non-graminoid vegetation), rock outcrops	C_4
Paspalum conjugatum P.J. Bergius	Savannas, patures, disturbed open areas	C_4
Paspalum decumbens Sw.	Forest edges, roadsides	C_4
Paspalum fasciculatum Willd. ex Flüggé	Bank of river, pastures and humid savannas, disturbed open areas	C_4
Paspalum foliiforme S. Denham	Savannas and open areas	C_4
Paspalum geminiflorum Steud.	Open areas	C_4
Paspalum hyalinum Nees ex Trin.	Savannas, *"herbazales"* (areas dominated by herbaceous, non graminoid vegetation), rock outcrops	C_4
Paspalum intermedium Munro ex Morong & Britton	Savannas, *"herbazales"* (areas dominated by herbaceous, non-graminoid vegetation), rock outcrops	C_4
Paspalum lanciflorum Trin.	Savannas, open areas	C_4
Paspalum laxum Lam.	River Banks	C_4
Paspalum melanospermum Desv. ex Poir.	Open areas	C_4
Paspalum minus E. Fourn.	Savannas, disturbed open areas	C_4
Paspalum notatum Flüggé	Savannas, pastures, disturbed open areas	C_4
Paspalum orbiculatum Poir.	Savannas, disturbed open areas	C_4
Paspalum pulchellum Kunth	Savannas, *"herbazales"* (areas dominated by herbaceous, non-graminoid vegetation), rock outcrops	C_4
Paspalum repens P.J. Bergius	Banks of rivers, lakes and swamps	C_4
Paspalum trinitense (Mez) S. Denham	Savannas	C_4
Paspalum virgatum L.	Wet, disturbed open areas	C_4

Taxon	Habitat	Photosynthetic Pathway
Trichanthecium nervosum (Lam.) Zuloaga & Morrone	Savannas, *"herbazales"* (areas dominated by herbaceous, non-graminoid vegetation)	C_3
Trichanthecium orinocanum (Luces) Zuloaga & Morrone	Humid savannas	C_3
Trichanthecium parvifolium (Lam.) Zuloaga & Morrone	Savannas, banks of rivers and lakes	C_3
Trichanthecium polycomum (Trin.) Zuloaga & Morrone	Savannas, *"herbazales"* (areas dominated by herbaceous, non-graminoid vegetations, rock outcrops	C_3
Trichanthecium pyrularium (Hitchc. & Chase) Zuloaga & Morrone	In wet, open areas	C_3
Reimarochloa acuta (Flüggé) Hitchc.	Savannas	C_4
Saccharum officinarum L.	Cultivated in open areas	C_4
Setaria parviflora (Poir.) Kerguélen	Savannas, conserved or disturbed open areas	C_4
Setaria sulcata Raddi	Shady places, river banks, forest edges	C_4
Setaria vulpiseta (Lam) Roem. & Schult.	Roadsides, forest edges	C_4
Sorghastrum setosum (Griseb.) Hitchc.	Savannas and open areas	C_4
Sorghum bicolor (L.) Moench.	Disturbed open areas, open fields	C_4
Steinchisma laxa (Sw.) Zuloaga	Savannas, disturbed open areas, pastures, roadsides	C_3
Stephostachys mertensii (Roth) Zuloaga & Morrone	Bank of river, lakes and swamps	C_3
Trachypogon vestitus Andersson	Savannas, *"herbazales"* (areas dominated by herbaceous, non-graminoid vegetation), rock outcrops	C_4
Tripsacum australe H.C. Cutler & E.S. Anderson	Savannas and open areas	C_4
Urochloa mutica (Forssk.) T.Q. Nguyen	Savannas, pastures, disturbed open areas	C_4
Zea mays L.	Cultivated in open areas	C_4
Pharus latifolius L.	Humid forest understory	C_3
Pharus virescens Döll	Humid forest understory	C_3